Mechanism and Machine Theory 44 (2009) 349–358

Contents lists available at ScienceDirect

Mechanism and Machine Theory

journal homepage: www.elsevier.com/locate/mechmt

The effects of dual row omnidirectional wheels on the kinematics of the Atlas spherical motion platform

A. Weiss, R.G. Langlois, M.J.D. Hayes *

Department of Mechanical and Aerospace Engineering, Carleton University, 1125 Colonel By Drive, Ottawa, ON, Canada K1S 5B6

ARTICLE INFO

Article history:
Received 24 October 2006
Received in revised form 18 January 2008
Accepted 14 March 2008
Available online 9 May 2008

Keywords:
Dual row omnidirectional wheels
Spherical motion platform
Kinematic analysis
Kinematic slip

ABSTRACT

A general modification to the kinematics model of the Atlas spherical orientation platform is presented. The Jacobian is augmented to include the effects of dual row omnidirectional wheels (i.e., two offset races of free spinning rollers). The results indicate that ignoring the offset between races can result in a significant error in the evaluation of the sphere angular velocity vector in response to a prescribed set of omnidirectional wheel velocities. The methodology presented in this paper is general and can be applied to the analysis of other mechanical systems employing dual row omnidirectional wheels.

1. Introduction

The Atlas spherical motion platform [1], shown in Fig. 1, is a novel conceptual design that allows unlimited angular displacements about any axis passing through the geometric centre of the sphere. Specifically, Atlas comprises a sphere resting on three omnidirectional wheels, which have rollers on their periphery allowing free motion in the direction perpendicular to the actuation direction (see Fig. 2). The omnidirectional wheels act as friction wheels to transmit the motion to the sphere, while not resisting motion in the direction orthogonal to the actuation direction. The kinematics of this platform have been derived by the authors for the case where the omnidirectional wheels are idealized to a single point of continuous contact with the sphere [2]. In reality, practical omnidirectional wheel design does not support such convenient assumptions. The nature of omnidirectional wheels necessitates discontinuities between the rollers that allow for the extra degree of freedom, leading essentially to two alternatives.

1. The first consists of a single row of rollers with some space between the rollers. This results in vibration during actuation due to changes in the local diameter of the omnidirectional wheel in gaps where no roller is present. However, the contact point, when present, remains in a single place. This type of wheel is commonly used in mobile robots [4,5]. Some attempts to solve the vibration issue have been made through either redesigning the omnidirectional wheels to minimize the gaps [6] or going through another level of smooth interface between the omnidirectional wheel and the point of contact by means of a smooth sphere between each actuating omnidirectional wheel and the other surface [7]. An alternative is the Mecanum wheel, where the rollers are at a 45° angle with respect to the main actuation axis of the wheel, instead of the more common 90° arrangement [8,9]. This solution, while reducing the normal vibrations, introduces more kinematic slip and lateral vibration into the system.

* Corresponding author.
E-mail addresses: aweiss2@connect.carleton.ca (A. Weiss), rlangloi@mae.carleton.ca (R.G. Langlois), jhayes@mae.carleton.ca (M.J.D. Hayes).

0094-114X/$ - see front matter © 2008 Elsevier Ltd. All rights reserved.
doi:10.1016/j.mechmachtheory.2008.03.013

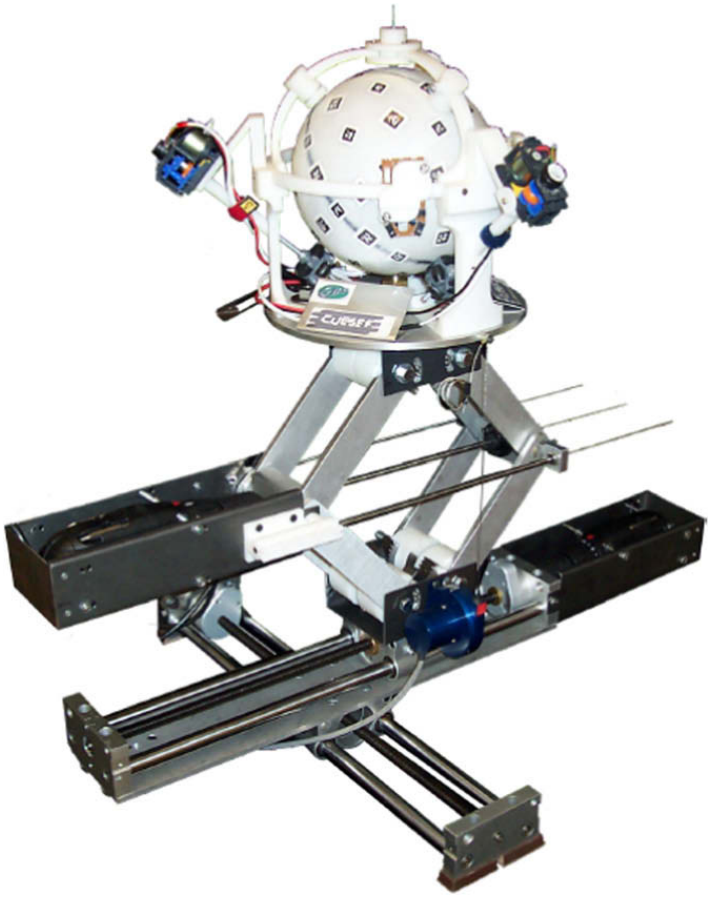

Fig. 1. The Atlas spherical motion platform table-top demonstrator attached to an $X - Y - Z$ linear motion platform.

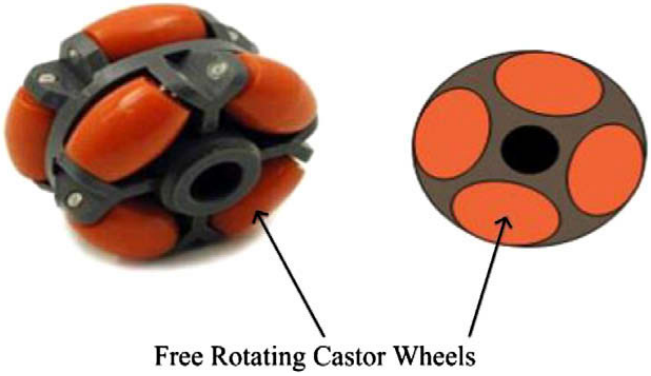

Fig. 2. A dual row omnidirectional wheel.

2. The second alternative consists of two rows of rollers (as shown in Fig. 2) arranged such that a roller is always in contact with the sphere. In this case, the point of contact on the sphere varies in time as the contact point switches from one roller to the other and back. This introduces a stepwise oscillation in the instantaneous contact point position vector, thereby altering the kinematics.

This paper focuses on the dual row case. Although dual row omnidirectional wheels have been used in previous applications, the shift of contact points has not been addressed, and an average contact point has always been assumed, explicitly or implicitly [9]. While in the case of mobile robots this contact point shift may be insignificant, when it comes to actuating a sphere, the errors in estimating the magnitude and direction of the resulting angular velocity vector of the sphere are more significant. This paper presents a generic analytical solution for the shifting contact point problem, demonstrates it using the current Atlas platform configuration, and formulates it in a convenient form.

2. The problem

While the kinematics for the Atlas platform have been developed in Ref. [2] for perfectly round omnidirectional wheels, here that basic assumption is removed. Instead, one of the more common solutions to the contact discontinuity problem, the use of dual row omnidirectional wheels will be treated. The dual row design aligns the rollers in two parallel rows, such that exactly when a roller on one row loses contact with the rolling surface the roller on the other row enters contact at the same point in time, thus maintaining roller contact at all times. Fig. 3 shows an imprint of a dual row omnidirectional wheel, in use in the Atlas demonstrator, on a flat surface. Attention is drawn to the fact that shifting one of the two parallel rows to align with the other yields a continuous straight line. This design indeed solves the contact gap problem, but introduces a new one: there is no longer a single point of contact. Rather, there are two alternating points of contact on the sphere. This change in the location of the contact point on the sphere alters the kinematics of the system and modifications to the kinematic model are necessary to improve the accuracy of the system kinematic and dynamic models. This is important for subsequent use in model-based control.

3. Refined kinematics model

The kinematics for the ideal case have been developed in Ref. [2]. The underlying concept there was to obtain a relationship between $\vec{\Omega}$, the angular velocity vector of the sphere, and ω_i, the angular speeds of the three omnidirectional wheels, that would account for zero kinematic slip between the sphere and the omnidirectional wheels. The condition is met by requiring that the projection of the velocities of the sphere at all contact points in the actuation direction of the omnidirectional wheel be the same, or, expressed mathematically

$$(\vec{\Omega} \times \vec{R}_i) \cdot \hat{v}_i = V_i, \tag{1}$$

where $\vec{R}_i$ is the position vector of contact point i, $\hat{v}_i$ is the vector of direction cosines of the omnidirectional wheel contact point velocities in the actuation directions, and V_i is the speed of omnidirectional wheel i at the contact point. This condition resulted in the following relationship

$$\vec{\Omega} = \mathbf{J}\vec{\omega}, \tag{2}$$

where $\vec{\omega}$ was defined as

$$\vec{\omega} = \begin{Bmatrix} \omega_1 \\ \omega_2 \\ \omega_3 \end{Bmatrix} \tag{3}$$

and $\mathbf{J}$ is the Jacobian of the architecture that, in the most general form, is

$$\mathbf{J} = \frac{1}{R} \begin{bmatrix} \widehat{\Omega}_1^{\mathrm{T}} \\ \widehat{\Omega}_2^{\mathrm{T}} \\ \widehat{\Omega}_3^{\mathrm{T}} \end{bmatrix}^{-1} \begin{bmatrix} r_1 & 0 & 0 \\ 0 & r_2 & 0 \\ 0 & 0 & r_3 \end{bmatrix}, \tag{4}$$

where r_i are the radii of the omnidirectional wheels and $\widehat{\Omega}_i$ are defined as the unit induced angular velocities, and defined as

$$\widehat{\Omega}_i = \widehat{R}_i \times \hat{v}_i \tag{5}$$

with $\widehat{R}_i$ being the direction cosines of the omnidirectional wheel contact point position vectors.

In the case of dual row omnidirectional wheels, the position vector $\vec{R}_i$ of the contact points alternates between two locations. We define six contact points (two per omnidirectional wheel) $\vec{R}_{ij}$, where the first index marks the omnidirectional wheel, and the second index marks the point of contact of a specific row on the wheel. This results in eight different combinations of possible simultaneous contact points:

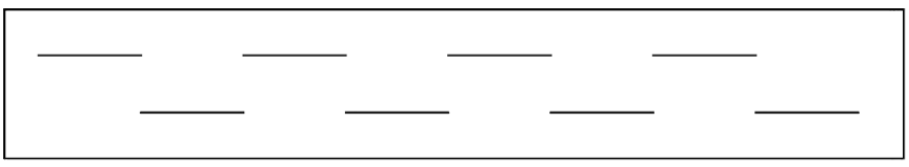

Fig. 3. The trace of a dual row omnidirectional wheel left when it rolls on a flat surface.

$$
\begin{matrix}
R_{11} & R_{21} & R_{31} \\
R_{11} & R_{21} & R_{32} \\
R_{11} & R_{22} & R_{31} \\
R_{11} & R_{22} & R_{32} \\
R_{12} & R_{21} & R_{31} \\
R_{12} & R_{21} & R_{32} \\
R_{12} & R_{22} & R_{31} \\
R_{12} & R_{22} & R_{32}
\end{matrix}.
$$

Now, since $\hat{v}_i$ remains the same as with the single-row case, the only change to $\widehat{\Omega}_i$ is due to the change from $\widehat{R}_i$ to $\widehat{R}_{ij}$, thus

$$\widehat{\Omega}_{ij} = \widehat{R}_{ij} \times \hat{v}_i \tag{6}$$

and so, we obtain eight Jacobians for the eight combinations above:

$$\mathbf{J}_{lmn} = \frac{1}{R}\begin{bmatrix} \widehat{\Omega}_{1l}^{\mathrm{T}} \\ \widehat{\Omega}_{2m}^{\mathrm{T}} \\ \widehat{\Omega}_{3n}^{\mathrm{T}} \end{bmatrix}^{-1} \begin{bmatrix} r_1 & 0 & 0 \\ 0 & r_2 & 0 \\ 0 & 0 & r_3 \end{bmatrix} \quad l,m,n = 1,2, \tag{7}$$

where the indices l, m, n determine the row in contact with the sphere on omnidirectional wheels 1, 2, and 3, respectively. Determining l, m, and n could be performed directly using sensors, or by simply integrating the angular velocities of each omnidirectional wheel independently, such that:

$$\phi_i = \int_0^t \omega_i \, \mathrm{d}t \tag{8}$$

and for $2N$ rollers per omnidirectional wheel, the indices may simply be calculated, using the integer floor values, as

$$l = \text{floor}\left[\frac{N\phi_1}{\pi} \mod 2\right] + 1, \tag{9}$$

$$m = \text{floor}\left[\frac{N\phi_2}{\pi} \mod 2\right] + 1, \tag{10}$$

$$n = \text{floor}\left[\frac{N\phi_3}{\pi} \mod 2\right] + 1. \tag{11}$$

This approach would require first evaluating the indices l, m, and n, and then calculating the angular velocity of the sphere, using the appropriate Jacobian.

4. Examples

The following examples show architectures that satisfy the necessary no-slip condition. The sphere has radius R, and each of the omnidirectional wheels has radius r, while the free-spinning rollers have radius r_r. The contact point details are illustrated in Fig. 4, where the dimensions of the rollers are exaggerated for clarity.

There is a deviation of $\pm\Delta\theta$ from the ideal contact point used in the evaluation of the Jacobian of the ideal case. It is clear from Fig. 4 that

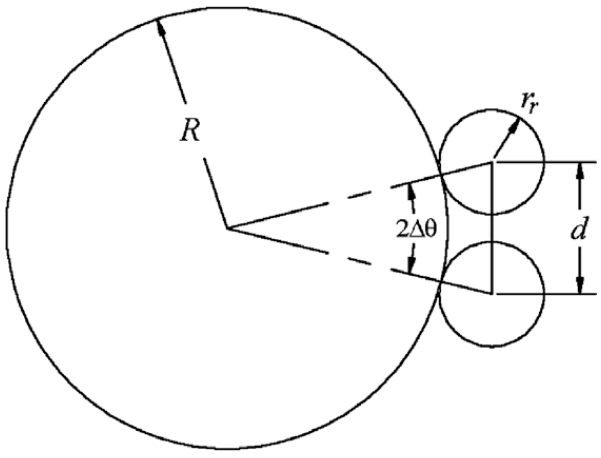

Fig. 4. The actual contact points on the Atlas sphere.

$$\sin\Delta\theta = \frac{\frac{d}{2}}{R+r_r} = \frac{d}{2(R+r_r)}, \tag{12}$$

thus

$$\cos\Delta\theta = \sqrt{1-\sin^2\Delta\theta} = \frac{1}{2(R+r_r)}\sqrt{4(R+r_r)^2-d^2}. \tag{13}$$

Utilizing these relations, it is clear that for any arbitrary angle θ

$$\begin{aligned}\sin(\theta\pm\Delta\theta) &= \frac{1}{2(R+r_r)}\left(\sqrt{4(R+r_r)^2-d^2}\sin\theta \pm d\cos\theta\right),\\ \cos(\theta\pm\Delta\theta) &= \frac{1}{2(R+r_r)}\left(\sqrt{4(R+r_r)^2-d^2}\cos\theta \mp d\sin\theta\right).\end{aligned} \tag{14}$$

4.1. The orthogonal case

Fig. 5 shows a case, where the omnidirectional wheels are mutually orthogonal. Thus, the position vectors of the three contact points for the ideal case are

$$\vec{R}_1 = R\hat{i};\quad \vec{R}_2 = R\hat{j};\quad \vec{R}_3 = R\hat{k}. \tag{15}$$

However, accounting for the angular deviation from the ideal contact point, the position vectors become:

$$\begin{aligned}\vec{R}_{11} &= R(\cos\Delta\theta\hat{i}+\sin\Delta\theta\hat{j}) = \frac{R}{2(R+r_r)}\left(\sqrt{4(R+r_r)^2-d^2}\hat{i}+d\hat{j}\right),\\ \vec{R}_{12} &= R(\cos\Delta\theta\hat{i}-\sin\Delta\theta\hat{j}) = \frac{R}{2(R+r_r)}\left(\sqrt{4(R+r_r)^2-d^2}\hat{i}-d\hat{j}\right),\\ \vec{R}_{21} &= R(\cos\Delta\theta\hat{j}+\sin\Delta\theta\hat{k}) = \frac{R}{2(R+r_r)}\left(\sqrt{4(R+r_r)^2-d^2}\hat{j}+d\hat{k}\right),\\ \vec{R}_{22} &= R(\cos\Delta\theta\hat{j}-\sin\Delta\theta\hat{k}) = \frac{R}{2(R+r_r)}\left(\sqrt{4(R+r_r)^2-d^2}\hat{j}-d\hat{k}\right),\\ \vec{R}_{31} &= R(\sin\Delta\theta\hat{i}+\cos\Delta\theta\hat{k}) = \frac{R}{2(R+r_r)}\left(d\hat{i}+\sqrt{4(R+r_r)^2-d^2}\hat{k}\right),\\ \vec{R}_{32} &= R(-\sin\Delta\theta\hat{i}+\cos\Delta\theta\hat{k}) = \frac{R}{2(R+r_r)}\left(-d\hat{i}+\sqrt{4(R+r_r)^2-d^2}\hat{k}\right).\end{aligned} \tag{16}$$

The direction cosines of the omnidirectional wheel contact point velocities in the actuation directions are [2]:

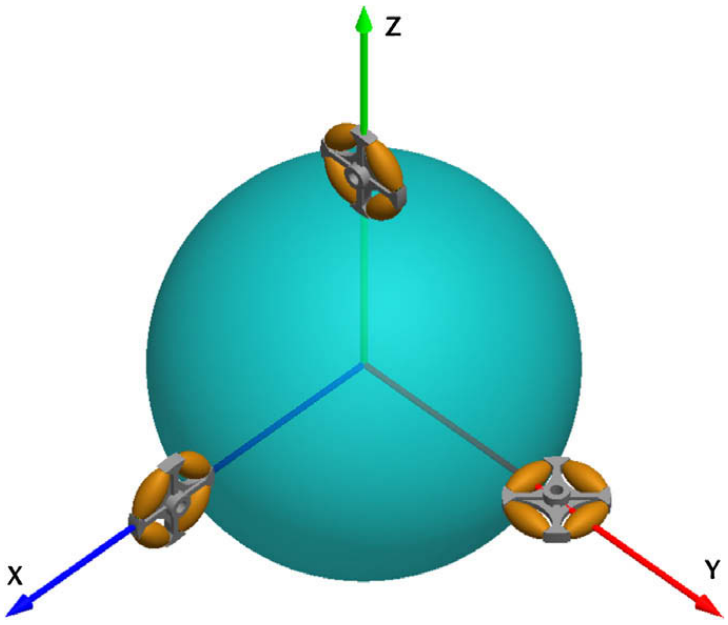

Fig. 5. Kinematic architecture for the orthogonal case.

$$\begin{aligned}\hat{v}_1 &= \hat{k},\\ \hat{v}_2 &= \hat{i},\\ \hat{v}_3 &= \hat{j}.\end{aligned} \tag{17}$$

Using these relations in Eq. (6), yields:

$$\begin{aligned}\widehat{\Omega}_{11} &= \frac{1}{2(R+r_r)}(d\hat{i} - \sqrt{4(R+r_r)^2 - d^2}\hat{j}),\\ \widehat{\Omega}_{12} &= \frac{1}{2(R+r_r)}\left(-d\hat{i} - \sqrt{4(R+r_r)^2 - d^2}\hat{j}\right),\\ \widehat{\Omega}_{21} &= \frac{1}{2(R+r_r)}\left(d\hat{j} - \sqrt{4(R+r_r)^2 - d^2}\hat{k}\right),\\ \widehat{\Omega}_{22} &= \frac{1}{2(R+r_r)}\left(-d\hat{j} - \sqrt{4(R+r_r)^2 - d^2}\hat{k}\right),\\ \widehat{\Omega}_{31} &= \frac{1}{2(R+r_r)}\left(-\sqrt{4(R+r_r)^2 - d^2}\hat{i} + d\hat{k}\right),\\ \widehat{\Omega}_{32} &= \frac{1}{2(R+r_r)}\left(-\sqrt{4(R+r_r)^2 - d^2}\hat{i} - d\hat{k}\right).\end{aligned} \tag{18}$$

Finally, the inverse Jacobian becomes:

$$\mathbf{J}_{lmn}^{-1} = \frac{\sqrt{4(R+r_r)^2 - d^2}}{2(R+r_r)}\mathbf{J}_{id}^{-1} + \frac{Rd}{2r(R+r_r)}\begin{bmatrix}(-1)^{l+1} & 0 & 0\\ 0 & (-1)^{m+1} & 0\\ 0 & 0 & (-1)^{n+1}\end{bmatrix}, \tag{19}$$

where $\mathbf{J}_{id}$ is the Jacobian for the ideal case:

$$\mathbf{J}_{id}^{-1} = \frac{R}{r}\begin{bmatrix}0 & -1 & 0\\ 0 & 0 & -1\\ -1 & 0 & 0\end{bmatrix}. \tag{20}$$

The orthogonal case is presented for discussion as it is convenient to study the essential difference between the single-race and dual race omnidirectional wheels. The first term in Eq. (19) indicates a slight reduction of the magnitude of $\vec{\Omega}$ in the original direction, while the second term reveals a more significant change in direction.

4.2. The Atlas platform

The current configuration of the Atlas spherical motion platform has the three omnidirectional wheels arranged on the edges of an equilateral triangle with an elevation angle of θ, as illustrated in Fig. 6. In this case:

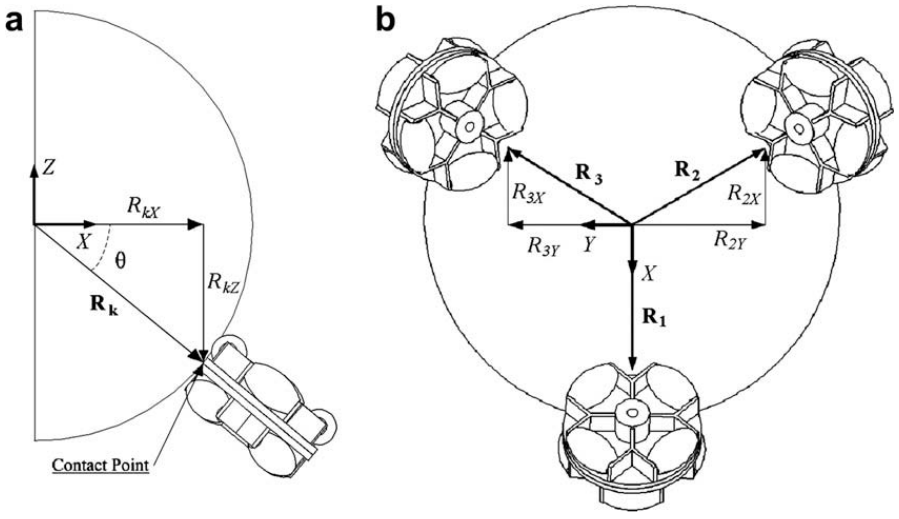

Fig. 6. Kinematic architecture for the Atlas sphere [3].

$$\begin{aligned}
\vec{R}_1 &= R(\cos\theta\hat{i} - \sin\theta\hat{k}),\\
\vec{R}_2 &= R\left(-\frac{1}{2}\cos\theta\hat{i} + \frac{\sqrt{3}}{2}\cos\theta\hat{j} - \sin\theta\hat{k}\right),\\
\vec{R}_3 &= R\left(-\frac{1}{2}\cos\theta\hat{i} - \frac{\sqrt{3}}{2}\cos\theta\hat{j} - \sin\theta\hat{k}\right).
\end{aligned} \tag{21}$$

Accounting for the change in the contact points, the new position vectors may be expressed as:

$$\begin{aligned}
\vec{R}_{11} &= R(\cos(\theta-\Delta\theta)\hat{i} - \sin(\theta-\Delta\theta)\hat{k}),\\
\vec{R}_{12} &= R(\cos(\theta+\Delta\theta)\hat{i} - \sin(\theta+\Delta\theta)\hat{k}),\\
\vec{R}_{21} &= R\left(-\frac{1}{2}\cos(\theta-\Delta\theta)\hat{i} + \frac{\sqrt{3}}{2}\cos(\theta-\Delta\theta)\hat{j} - \sin(\theta-\Delta\theta)\hat{k}\right),\\
\vec{R}_{22} &= R\left(-\frac{1}{2}\cos(\theta+\Delta\theta)\hat{i} + \frac{\sqrt{3}}{2}\cos(\theta+\Delta\theta)\hat{j} - \sin(\theta+\Delta\theta)\hat{k}\right),\\
\vec{R}_{31} &= R\left(-\frac{1}{2}\cos(\theta-\Delta\theta)\hat{i} - \frac{\sqrt{3}}{2}\cos(\theta-\Delta\theta)\hat{j} - \sin(\theta-\Delta\theta)\hat{k}\right),\\
\vec{R}_{32} &= R\left(-\frac{1}{2}\cos(\theta+\Delta\theta)\hat{i} - \frac{\sqrt{3}}{2}\cos(\theta+\Delta\theta)\hat{j} - \sin(\theta+\Delta\theta)\hat{k}\right).
\end{aligned} \tag{22}$$

The direction cosines of the omnidirectional wheel contact point velocities in the actuation directions are [2]:

$$\begin{aligned}
\hat{v}_1 &= \hat{j},\\
\hat{v}_2 &= -\frac{\sqrt{3}}{2}\hat{i} - \frac{1}{2}\hat{j},\\
\hat{v}_3 &= \frac{\sqrt{3}}{2}\hat{i} - \frac{1}{2}\hat{j}.
\end{aligned} \tag{23}$$

Utilizing the relations shown in Eqs. (14), (22), and (23) in Eq. (6), the expressions for the unit vectors identifying the directions of the sphere's angular velocity components induced by the individual omnidirectional wheels are

$$\begin{aligned}
\widehat{\Omega}_{11} &= \frac{1}{2(R+r_r)}\left[\left(\sqrt{4(R+r_r)^2-d^2}\sin\theta - d\cos\theta\right)\hat{i} + \left(\sqrt{4(R+r_r)^2-d^2}\cos\theta + d\sin\theta\right)\hat{k}\right],\\
\widehat{\Omega}_{12} &= \frac{1}{2(R+r_r)}\left[\left(\sqrt{4(R+r_r)^2-d^2}\sin\theta + d\cos\theta\right)\hat{i} + \left(\sqrt{4(R+r_r)^2-d^2}\cos\theta - d\sin\theta\right)\hat{k}\right],\\
\widehat{\Omega}_{21} &= \frac{1}{2(R+r_r)}\left[-\frac{1}{2}\left(\sqrt{4(R+r_r)^2-d^2}\sin\theta - d\cos\theta\right)\hat{i} + \frac{\sqrt{3}}{2}\left(\sqrt{4(R+r_r)^2-d^2}\sin\theta - d\cos\theta\right)\hat{j}\right.\\
&\quad \left. + \left(\sqrt{4(R+r_r)^2-d^2}\cos\theta + d\sin\theta\right)\hat{k}\right],\\
\widehat{\Omega}_{22} &= \frac{1}{2(R+r_r)}\left[-\frac{1}{2}\left(\sqrt{4(R+r_r)^2+d^2}\sin\theta + d\cos\theta\right)\hat{i} + \frac{\sqrt{3}}{2}\left(\sqrt{4(R+r_r)^2+d^2}\sin\theta + d\cos\theta\right)\hat{j}\right.\\
&\quad \left. + \left(\sqrt{4(R+r_r)^2-d^2}\cos\theta - d\sin\theta\right)\hat{k}\right],\\
\widehat{\Omega}_{31} &= \frac{1}{2(R+r_r)}\left[-\frac{1}{2}\left(\sqrt{4(R+r_r)^2-d^2}\sin\theta - d\cos\theta\right)\hat{i} - \frac{\sqrt{3}}{2}\left(\sqrt{4(R+r_r)^2-d^2}\sin\theta - d\cos\theta\right)\hat{j}\right.\\
&\quad \left. + \left(\sqrt{4(R+r_r)^2-d^2}\cos\theta + d\sin\theta\right)\hat{k}\right],\\
\widehat{\Omega}_{32} &= \frac{1}{2(R+r_r)}\left[-\frac{1}{2}\left(\sqrt{4(R+r_r)^2+d^2}\sin\theta + d\cos\theta\right)\hat{i} - \frac{\sqrt{3}}{2}\left(\sqrt{4(R+r_r)^2-d^2}\sin\theta + d\cos\theta\right)\hat{j}\right.\\
&\quad \left. + \left(\sqrt{4(R+r_r)^2-d^2}\cos\theta - d\sin\theta\right)\hat{k}\right].
\end{aligned} \tag{24}$$

Finally, the inverse Jacobian becomes:

$$\mathbf{J}^{-1}_{lmn} = \frac{R}{r}\frac{\sqrt{4(R+r_r)^2-d^2}}{2(R+r_r)}\begin{bmatrix}\sin\theta & 0 & \cos\theta\\ -\frac{1}{2}\sin\theta & \frac{\sqrt{3}}{2}\sin\theta & \cos\theta\\ -\frac{1}{2}\sin\theta & -\frac{\sqrt{3}}{2}\sin\theta & \cos\theta\end{bmatrix} + \frac{R}{r}\frac{d}{2(R+r_r)}\begin{bmatrix}(-1)^l\cos\theta & 0 & (-1)^{l+1}\sin\theta\\ (-1)^{m+1}\frac{1}{2}\cos\theta & (-1)^m\frac{\sqrt{3}}{2}\cos\theta & (-1)^{m+1}\sin\theta\\ (-1)^{n+1}\frac{1}{2}\cos\theta & (-1)^{n+1}\frac{\sqrt{3}}{2}\cos\theta & (-1)^{n+1}\sin\theta\end{bmatrix}. \tag{25}$$

The inverse Jacobian for the ideal system is [2]

$$\mathbf{J}^{-1} = \frac{R}{r}\begin{bmatrix} \sin\theta & 0 & \cos\theta \\ -\frac{1}{2}\sin\theta & \frac{\sqrt{3}}{2}\sin\theta & \cos\theta \\ -\frac{1}{2}\sin\theta & -\frac{\sqrt{3}}{2}\sin\theta & \cos\theta \end{bmatrix}. \tag{26}$$

For the dual row system the inverse Jacobian is

$$\mathbf{J}_{lmn}^{-1} = \frac{\sqrt{4(R+r_r)^2 - d^2}}{2(R+r_r)}\mathbf{J}^{-1} + \frac{R}{r}\Delta\mathbf{J}', \tag{27}$$

where $\mathbf{J}^{-1}$ is the inverse of the Jacobian for the ideal case and $\Delta\mathbf{J}'$ is the correction component for the contact point change, such that

$$\Delta\mathbf{J}' = \frac{d}{2(R+r_r)}\begin{bmatrix} (-1)^l\cos\theta & 0 & (-1)^{l+1}\sin\theta \\ (-1)^{m+1}\frac{1}{2}\cos\theta & (-1)^m\frac{\sqrt{3}}{2}\cos\theta & (-1)^{m+1}\sin\theta \\ (-1)^{n+1}\frac{1}{2}\cos\theta & (-1)^{n+1}\frac{\sqrt{3}}{2}\cos\theta & (-1)^{n+1}\sin\theta \end{bmatrix}. \tag{28}$$

This last term is the only one required to be reevaluated as it is the only one that may vary in time. The Jacobian of the system is therefore

$$\mathbf{J}_{lmn} = (\mathbf{J}^{-1} + \frac{R}{r}\Delta\mathbf{J}')^{-1}. \tag{29}$$

5. Numerical results

Some numerical examples have been performed in order to demonstrate the importance of the suggested correction to the Jacobian. The program developed for this purpose evaluates the resulting angular velocity vector for a few sets of time-varying inputs, for both the original Jacobian developed for the ideal case, and for the corrected Jacobian suggested in this paper. The magnitude and the direction of the resulting angular velocity vectors are evaluated and compared for both cases. The reference platform for the numerical experiment is an Atlas platform as described in the previous section, with an elevation angle of $\theta = 40°$, and the following design parameters:

$$R = 15\text{ cm}, \quad r_r = 4.85\text{ mm}, \quad d = 12.5\text{ mm}, \quad r = 25\text{ mm}, \quad 2N = 16.$$

The input is a set of angular speeds of the three omnidirectional wheels, prescribed to illustrate a variety of cases. The inputs are described in Table 1.

The prescribed input was selected to demonstrate cases with various ratios among the omnidirectional wheels' angular speeds. The first step was intended for creating a slight misalignment such that the experiment will have a starting point where not all omnidirectional wheels are in the same phase.

Fig. 7 shows the orientation error [°] of the angular velocity vector $\vec{\Omega}$ of the sphere and the error [%] in the magnitude of $\vec{\Omega}$. The orientation error is defined as the angle between the two resulting angular velocity vectors:

$$\epsilon = \cos^{-1}\left(\frac{\vec{\Omega}_{id}\cdot\vec{\Omega}}{\|\vec{\Omega}_{id}\|\|\vec{\Omega}\|}\right), \tag{30}$$

Table 1
Prescribed omnidirectional wheel inputs

Time (s)	ω_1 (rad/s)	ω_2 (rad/s)	ω_3 (rad/s)
0	1	0	0
0.1	1	1	1
1	1	2	2
2	2	1	1
3	2	1	2
4	0	0	1
5	1	0	0
6	0	1	0
7	1	2	3
8	2	1	3
9	1	3	2
10	2	3	1
11	3	1	2
12	3	2	1
13	0	0	0

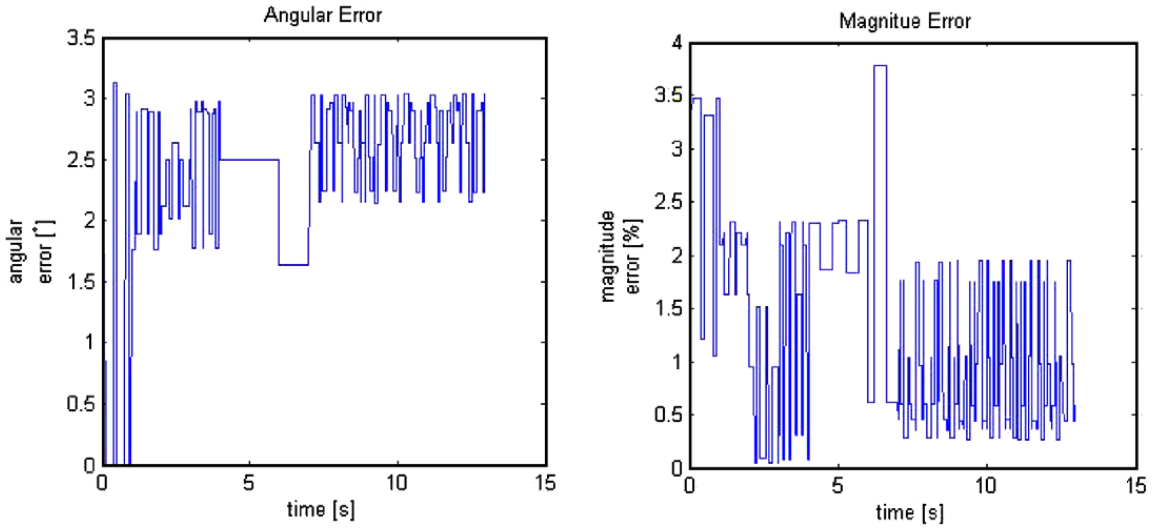

Fig. 7. Errors in angle and magnitude of the sphere angular velocity vector.

where $\vec{\Omega}_{id}$ is the resultant angular velocity vector for the ideal single-row case. It is clear from the results that there are both magnitude and direction errors that are generally non-zero. The magnitude error peaks at 3.8%, for the selected input set. The angular deviation, which is the angle between the angular velocity vector of the sphere, calculated using the augmented Jacobian, and the angular velocity vector of the sphere calculated using the ideal case Jacobian, as demonstrated in Eq. (30) is also generally non-zero, and peaks at an angle of 3.2°. The zero case only exists when the prescribed angular speeds of all three omnidirectional wheels are the same, which translates to a rotation about the Z-axis of the sphere, as long as all omnidirectional wheels are touching with the same race. The initial intentional misalignment is used to prevent this unique case, and demonstrate the more general case for which the augmented Jacobian presented above was developed.

6. Conclusion

The problem of shifting contact points because of the nature of the dual row omnidirectional wheels in current use in the Atlas spherical orienting platform has a closed form solution, which is presented in this paper for the first time. The solution requires either a sensing process or an integration process to determine the current contact points, which determines the correct Jacobian to be used. In the case of the Atlas configuration, the eight Jacobian matrices could be reduced to an ideal matrix $\mathbf{J}$ and a correction matrix $\Delta\mathbf{J}'$ that needs to be reevaluated after each integration step. This correction matrix can either be viewed as an actual correction term, or as the error in the evaluation of $\vec{\Omega}$ using the ideal Jacobian developed in Ref. [2]. It is also worth noting that the presented solution reduces to the ideal solution for the case of $d = 0$, so that it can be used as a more general expression for the kinematics of the system.

A closer look at Eqs. (19) and (25) from the examples reveals that one can generalize the Jacobian of a system comprising of three identical dual row omnidirectional wheels:

$$\mathbf{J}^{-1}_{lmn} = \frac{R}{r}\frac{1}{2(R+r_r)}\left\{\sqrt{4(R+r_r)^2-d^2}\begin{bmatrix}\widehat{\Omega}_1^{\mathrm{T}}\\ \widehat{\Omega}_2^{\mathrm{T}}\\ \widehat{\Omega}_3^{\mathrm{T}}\end{bmatrix} - d\begin{bmatrix}(-1)^l\widehat{R}_1^{\mathrm{T}}\\ (-1)^m\widehat{R}_2^{\mathrm{T}}\\ (-1)^n\widehat{R}_3^{\mathrm{T}}\end{bmatrix}\right\} \quad l,m,n = 1,2. \tag{31}$$

Since $\widehat{R}_i$ is orthogonal to $\widehat{\Omega}_i$ by definition, the only way to avoid the directional error of $\vec{\Omega}$ is to set $d = 0$, thereby reducing the solution to a single row.

While in the case of mobile robots this problem is rarely considered, the results presented herein suggest that the effects may cause non-negligible errors. These results suggest that when actuating a sphere, the errors in estimating the magnitude and direction of the resulting angular velocity vector of the sphere may be significant.

References

[1] M.J.D. Hayes, R.G. Langlois, A novel kinematic architecture for six DOF motion platforms, CSME Transactions 29 (4) (2005) 701–709 (Special edition).
[2] A. Weiss, R.G. Langlois, M.J.D. Hayes, Atlas: a six degree-of-freedom singularity-free motion platform with unbounded rotation that is decoupled from translation, Private communication, available upon request from the corresponding author, October 26, 2006.
[3] J.B. Holland, M.J.D. Hayes, R.G. Langlois, A slip model for the spherical actuation of the Atlas motion platform, CSME Transactions 29 (4) (2005) 711–720 (Special edition).
[4] Y.P. Leow, K.H. Low, W.K Loh, Kinematic modelling and analysis of mobile robots with omni-directional wheels, in: Proceedings of the 7th International Conference on Control, Automation, Robotics and Vision, ICARCV 2002, 2002, pp. 820–825.
[5] R. Williams, D. Carter, P. Gallina, G. Rosati, Dynamics model with slip for wheeled omni-directional robots, IEEE Transactions on Robotic and Automation 18 (3) (2002) 285–293.

[6] J.B. Song, K.S. Byun, Design and control of a four wheeled omnidirectional mobile robot with steerable omnidirectional wheels, Journal of Robotic Systems 21 (4) (2004) 193–208 (April).
[7] L. Ferriere, B. Raucent, ROLLMOBS, a new universal wheel concept, in: Proceedings of the 1998 IEEE International Conference on Robotics and Automation, 1998, pp. 1877–1882 (May).
[8] S.L. Dickerson, Control of an omni-directional robotic vehicle with mecanum wheels, in: Proceedings of the 1991 IEEE International Conference on Robotics and Automation, 1991, 323–328.
[9] J. Agullo, S. Cardona, J. Vivancos, Dynamics of vehicle with directionally sliding wheels, Mechanism and Machine Theory 24 (1) (1989) 53–60.